Nitritation membrane-based process for enhancing nitrogen removal and PHA production from waste-activated sludge

Mineo, Antonio; Van Loosdrecht, Mark M.C.; Mannina, Giorgio

DOI
10.1016/j.psep.2025.107802

Publication date
2025

Document Version
Final published version

Published in
Process Safety and Environmental Protection

Process Safety and Environmental Protection 202 (2025) 107802

Contents lists available at ScienceDirect

Process Safety and Environmental Protection

journal homepage: www.journals.elsevier.com/process-safety-and-environmental-protection

Nitritation membrane-based process for enhancing nitrogen removal and PHA production from waste-activated sludge

Antonio Mineo [a,*], Mark M.C. Van Loosdrecht [b], Giorgio Mannina [a]

[a] Engineering Department, Palermo University, Viale delle Scienze ed. 8, Palermo 90128, Italy
[b] Department of Biotechnology, Delft University of Technology, Van der Maasweg 9, Delft 2629 Hz, the Netherlands

ARTICLE INFO

Keywords:
Biopolymers
Bio-solids
Greenhouse gas emission
Waste activated sludge
Wastewater treatment

ABSTRACT

This work explores the combined application of biological nitrogen removal and polyhydroxyalkanoate (PHA) synthesis within the operational framework of a wastewater treatment plant (WWTP), employing waste-activated sludge as both the microbial inoculum and carbon source. Consistent and high-yield PHA production was achieved through a membrane-assisted microbial enrichment strategy, carried out in alternating aerobic and anoxic conditions, comprising a nitritation sequencing batch reactor (N-SBR), a membrane-based selection reactor (S-SBR), and a continuously operated PHA accumulation unit (A-SBR). The A-SBR reached 40–44 % w/w of PHA for about 70 days, while the storage yield was within 0.32–0.53 g COD_{PHA} g^{-1} COD_{VFA}. The system maintained high efficiency despite the C/N variation around 2 and 6 g COD g^{-1} N. Nitrous oxide (N_2O) was monitored to assess the direct greenhouse gas (GHG) emissions. The N-SBR achieved the peak concentration of 0.62 ± 0.08 mg N_2O-N L^{-1} during period I (C/N 2), while the highest emission factor of 0.49 ± 0.08 % was reached during period IV (C/N 6). This research highlights the benefits of integrating PHA production into WWTP operations, which involves recovering resources while meeting stricter nutrient removal and environmental impact standards. Future work should focus on optimizing nutrient removal and mitigating GHG emissions to fully meet the requirements of evolving urban wastewater treatment regulations.

1. Introduction

Biopolymers, such as polyhydroxyalkanoates (PHA), have rapidly gained recognition as high-value resources when recovered from solid waste. The increasing demand for sustainable waste management and resource recovery has increased interest in waste-activated sludge (WAS) based PHA production (Awasthi et al., 2023; Zhang and Liu, 2022). Being a major waste of wastewater treatment plant (WWTP) operations, WAS offers a substrate rich in organic matter but is hardly exploitable for producing PHA without proper pre-treatments (Zhang et al., 2018; Chaudhry et al., 2011). The integration of PHA production into conventional WWTPs represents a promising step toward the development of water resource recovery facilities (WRRFs), potentially enhancing both resource efficiency and process sustainability.

PHA production can be coupled with a complete nitrogen (N) removal process through a preliminary nitritation step by applying aerobic/anoxic enrichment (AE/AN) (Frison et al., 2015a). The same strategy, involving the use of a specific nitritation reactor, has been explored by Conca et al. (2020) (Conca et al., 2020), who validated the process at pilot scale. The same enrichment strategy has also been adopted by Basset et al. (2016) (Basset et al., 2016), who explored using a single reactor process in which the NO_x species produced during the aerobic feast serve as an electron acceptor during the anoxic famine. The same process was also tested on a laboratory scale, highlighting that no significant difference was observed between nitrate and nitrite as electron acceptors in the process (Tu et al., 2019; Liu et al., 2023). In all the previous studies cited, the accumulation was carried out in batch mode, with the process length fixed. However, this approach would still require improvement to achieve a continuous process that could be more easily implemented on larger scales (Guo et al., 2024). The N removal-PHA production process, though nitrite/nitrate denitrification, offers several advantages due to the possibility of coupling it to conventional WWTP operation treating high N load influents. At the same time, despite the high removal efficiency achievable, a consistent concentration of N will remain in the effluent waters, posing a potential risk to receiving water bodies.

The C/N ratio effect was recently assessed in AE/AN enrichment in a pilot plant fed by real wastewater/WAS (Mineo et al., 2024). System

* Corresponding author.
E-mail address: antonio.mineo01@unipa.it (A. Mineo).

https://doi.org/10.1016/j.psep.2025.107802
Received 30 May 2025; Received in revised form 28 August 2025; Accepted 29 August 2025
Available online 1 September 2025

performance was evaluated under varying external C/N ratios, with a particular focus on the environmental implications of nitrous oxide (N_2O) emissions. Effluent quality characterization was limited, as the primary objective was to investigate nitrogen removal within the mainline process, excluding tertiary treatment steps. Consequently, the evaluation does not fully capture the extent of contaminant removal. Another previous study introduced a membrane bioreactor (MBR) in the enrichment process by applying aerobic dynamic feeding (Mineo et al., 2025). Despite the high removal efficiencies obtained, complete N removal could not be achieved due to the lack of a denitrification phase. Today's environmental challenges, posed by climate change, have further motivated actions to preserve the environment and human health. The revision of the Urban Wastewater Treatment Directive imposes stricter limits on nitrogen (N) and phosphorus (P) concentrations in the effluent, as well as the monitoring of greenhouse gas (GHG) emissions (European Parliament, 2024). Moreover, the directive hardly promotes the practice of water reuse, almost as a mandatory requirement for larger WWTPs, as water scarcity has become a severe global threat (He and Rosa, 2023). However, a revamp of existing WWTPs will be required to produce effluent that can be reused following the new directive limits. If the strict requirements are respected, this necessary revamping could be the key step in fostering PHA production implementation within WWTPs.

To test the efficiency of the AE/AN enrichment in the context of the new EU Directive, a membrane bioreactor (MBR) was applied to the main effluent stream of the PHA production process, the selection reactor. The sludge withdrawn from the reactor was used as substrate in a continuous accumulation reactor run in parallel. The study's goal was to monitor and test the efficiency of the aforementioned process, utilising the nitritation reactor for the first time in the membrane-based enrichment process and a continuous PHA accumulation reactor. Given their relevance, direct GHG emissions were monitored to assess the environmental footprint of the proposed configuration, alongside sCOD, nitrogen and phosphorus removal efficiencies and PHA production performance.

2. Materials and methods

2.1. PHA production plant layout

The pilot plant is located at the WRRF of Palermo University (Mannina et al., 2021). The PHA line operates as the sludge treatment train within the mainstream wastewater treatment pilot plant. It comprises four units, beginning with a 200 L fermenter coupled with an ultrafiltration (UF) module to recover volatile fatty acids (VFAs). The nitritation sequencing batch reactor (N-SBR) is the second unit designed to produce a nitrite- and nitrate-rich effluent (working volume: 30 L). The third unit, a selection sequencing batch reactor (S-SBR) with a working volume of 50 L, is designed to enrich the mixed microbial culture through a feast/famine regime. At the onset of the feast phase, the VFA recovered from the fermenter is fed under aerobic conditions. The nitrites and nitrates-rich liquid produced in the N-SBR is fed during the famine phase in the S-SBR, which is carried out in anoxic conditions. The last unit is the accumulation SBR (A-SBR), which is periodically inoculated with waste sludge from the S-SBR and operates continuously in a feast-on-demand mode automatically controlled (Mineo et al., 2023). All reactors were inoculated with WAS sourced from the mainstream wastewater treatment line. The experimental period was characterised by four C/N ratios (expressed as g COD g^{-1} N), based on the characteristics of the fermented sludge liquid reported in Table 1: period I – 2 COD/N; period II – 3 COD/N; period III – 4; and period IV – 6 COD/N. Variations in the characteristics of the fermented sludge liquor reflected seasonal fluctuations in the composition of the WAS, driven by changes in campus wastewater related to canteen activity and dormitory occupancy.

2.2. VFA production

Acidogenic fermentation of WAS was carried out in a continuously stirred tank reactor, operated at a hydraulic and sludge retention time (HRT and SRT, respectively) of 5 days. Following fermentation, the sludge mixture was filtered using a hollow fiber membrane within the 40 L UF unit. No pre-treatment was applied to the WAS, while pH and temperature were monitored using a WTW SenTix probe. The liquid obtained from the fermented WAS filtration was used as feedstock for the other reactors in the pilot plant, and its characteristics are reported in Table 1.

2.3. Nitritation reactor

The N-SBR was designed to achieve partial ammonia oxidation, generating electron acceptors for use during the famine phase of the S-SBR. It was fed with fermented sludge liquor, similarly to the S-SBR. The cycle duration ranged from 3.5 to 4 h, depending on operational conditions, and consisted of feeding (15 min), aerobic reaction (2.5–3 h), settling (30 min) and effluent withdrawal (15 min). The effluent was collected and subsequently used as feedstock for the S-SBR. The operational conditions of the N-SBR are reported in Table 2.

2.4. Selection reactor

The S-SBR was operated to enrich the microbial community in PHA-accumulating organisms. Each cycle included VFA feeding, an aerobic feast phase, addition of N-SBR effluent, an anoxic famine phase and effluent withdrawal via membrane filtration. The total cycle duration was approximately 10 h, with the feast phase lasting 1–3 h, depending

Table 1
Average features of the fermented waste-activated sludge filtration liquid.

Parameter	U.M	Period I	Period II	Period III	Period IV
sCOD	mg L^{-1}	215.51 ± 69.56	373.92 ± 36.58	470.84 ± 23.67	363.12 ± 105.40
VFA	mg COD L^{-1}	98.89 ± 29.90	131.93 ± 14.64	193.94 ± 29.97	104.99 ± 61.04
Acetic acid	mg COD L^{-1}	51.52 ± 46.18	121.82 ± 13.29	179.11 ± 28.57	96.93 ± 56.98
Propionic acid	mg COD L^{-1}	10.90 ± 1.89	9.01 ± 7.42	6.32 ± 5.07	6.59 ± 6.18
Iso-butyric acid	mg COD L^{-1}	0.12 ± 0.07	0.08 ± 0.04	0.64 ± 0.24	0.07 ± 0.03
Butyric acid	mg COD L^{-1}	1.10 ± 0.97	1.56 ± 1.12	10.86 ± 8.02	2.21 ± 1.21
Iso-valeric acid	mg COD L^{-1}	0.15 ± 0.05	0.07 ± 0.04	-	0.16 ± 0.07
Valeric acid	mg COD L^{-1}	35.04 ± 30.20	0.61 ± 0.21	-	0.21 ± 0.09
Hexanoic acid	mg COD L^{-1}	0.07 ± 0.05	-	-	-
VFA/sCOD	mg COD_{VFA} mg COD^{-1}	0.46 ± 0.05	0.36 ± 0.05	0.41 ± 0.06	0.27 ± 0.08
NH_4^+-N	mg N L^{-1}	115.24 ± 10.69	115.30 ± 9.57	107.75 ± 4.08	56.99 ± 21.59
NO_2^--N	mg N L^{-1}	0.04 ± 0.01	0.33 ± 0.20	0.51 ± 0.08	0.06 ± 0.06
NO_3^--N	mg N L^{-1}	0.36 ± 0.02	0.52 ± 0.18	0.82 ± 0.34	0.31 ± 0.28
PO_4^{3-}-P	mg P L^{-1}	23.01 ± 3.95	11.04 ± 6.29	8.52 ± 4.52	10.21 ± 4.88

Soluble chemical oxygen demand (sCOD); Ammonium (NH_4^+-N); Nitrites (NO_2^--N); Nitrates NO_3^--N); Orto-phosphate (PO_4^{3-}-P)

Table 2
Average operational conditions of the nitritation reactor.

Parameter	U.M	Period I	Period II	Period III	Period IV
Influent C/N	g COD g N^{-1}	1.90 ± 0.47	3.36 ± 0.52	4.16 ± 0.63	5.61 ± 1.38
F/M	kg BOD kg SS^{-1} d^{-1}	0.11 ± 0.04	0.18 ± 0.03	0.23 ± 0.06	0.17 ± 0.08
SRT	days	5.91 ± 2.05	6.01 ± 2.53	6.03 ± 2.24	5.11 ± 2.32
OLR	kg COD m^{-3} d^{-1}	0.32 ± 0.10	0.56 ± 0.05	0.66 ± 0.09	0.47 ± 0.18
NLR	kg N m^{-3} d^{-1}	0.17 ± 0.02	0.17 ± 0.01	0.16 ± 0.01	0.09 ± 0.03
TSS	g L^{-1}	1.20 ± 0.11	1.25 ± 0.20	1.21 ± 0.18	1.15 ± 0.18
VSS	g L^{-1}	0.87 ± 0.11	0.94 ± 0.19	0.88 ± 0.12	0.84 ± 0.07
Temperature	℃	18 ± 3	23 ± 2	27 ± 4	28 ± 2

Food to microorganism ratio (F/M); Organic Loading Rate (OLR); Nitrogen Loading Rate (NLR); Total suspended solids (TSS); Volatile suspended solids (VSS)

on process dynamics. The transition to the famine phase was triggered when dissolved oxygen (DO) levels reached a plateau, indicating VFA depletion. DO and temperature were monitored using a WTW FDO 925–3 probe. The operational conditions for the S-SBR are reported in Table 3.

2.5. Accumulation reactor

PHA accumulation was conducted in a 20 L tempered glass reactor operated under a feed-on-demand strategy. WAS from the S-SBR served as a periodic inoculum, enabling continuous operation. The reactor was aerobically fed with VFAs produced in the fermenter, with DO used as a control variable via an automated system (Mineo et al., 2023). The substrate was resupplied upon VFA depletion, as indicated by a decrease in DO. After several feedings, the aeration was stopped, allowing the sludge to settle for 20 min. The supernatant was then removed, and the next cycle was initiated by reactivating the air supply. Once the sludge took 2 h to consume, the substrate was fed, part was withdrawn, and the S-SBR wasted sludge was fed. The amounts of sludge withdrawn and fed were based on maintaining a fixed concentration of 1 g L^{-1} of TSS in the reactor.

2.6. Analytical methods and calculations

Liquid samples were collected twice a week in the fermenter to analyse sCOD, VFAs, NH_4^+-N, and PO_4^{3-}-P. For the N-SBR and S-SBR, influent and effluent samples were analyzed twice weekly for sCOD, NH_4^+-N, PO_4^{3-}-P, NO_3^--N and NO_2^--N.

Mixed liquor was sampled weekly to quantify the dissolved N_2O concentration, following the approach of Mannina et al. (2018a). Samples were centrifuged at 8000 rpm for 20 min. Seventy-five millilitres of supernatant were transferred to 125 mL glass bottles and acidified with 1 mL of 2 N H_2SO_4. Bottles were sealed and continuously mixed for 24 h to establish liquid–gas equilibrium. The headspace was then sampled to determine the dissolved N_2O concentration. Gaseous N_2O was quantified by directly sampling the reactors' headspace via the installed covers and sampling ports. Dissolved and gaseous N_2O were analysed in duplicate using a gas chromatograph (Agilent 8860) equipped with a packed column (Popapak-Q 80/100 mesh, 6 ft - 1/8" x 2.1 mm) and an electron-capture detector. The N_2O emission factor (EF_{N2O}) was calculated according to the literature (Tsuneda et al., 2005), as reported by Eq. 1:

$$EF_{N2O} = \frac{N_2O - N_g/HRT_{HS} + N_2O - N_d/HRT}{TN} \quad (1)$$

where N_2O-N_g and N_2O-N_d are the gaseous and dissolved nitrous oxide concentrations, respectively, HRT is the pilot-plant hydraulic retention time, HRT_{HS} is the retention time in the tank headspace, and TN is the total nitrogen concentration in the influent flow.

In the A-SBR, mixed liquor was sampled twice weekly to determine PHA content, defined as the sum of polyhydroxybutyrate (PHB) and polyhydroxyvalerate (PHV) (Conca et al., 2020).

Standard methods (Rice and Bridgewater, 2012) were employed to analyze sCOD, TCOD, NH_4^+-N, PO_4^{3-}-P, NO_3^--N, NO_2^--N, TSS and VSS. VFA were quantified following the protocol described in the literature (Montiel-Jarillo et al., 2021). A gas chromatograph with a DB-FFAA column (MEGA-1, 30 m× 0.32 mm× 5μm) was used to determine VFA concentrations, while a Restek Stabilwax column (30 m x 0.53 mm×1.00 μm) was used to determine the PHA concentration (Mannina et al., 2019). PHA concentration was expressed as the percentage of PHA per biomass unit (% gPHA g^{-1}VSS). The PHA storage yield was calculated as the mass of PHA per VFA supplied ($gCOD_{PHA}$ $g^{-1}COD_{VFA}$). Oxidation stoichiometries of 1.67 g COD g^{-1} for PHB and 1.92 g COD g^{-1} for PHV were applied, while VFA conversion factors followed the values reported by Yuan et al. (2011) (Yuan et al., 2011). N-SBR performance was evaluated through the nitrite accumulation rate (NAR) (Kowal et al., 2022), as reported by Eq. 2:

$$NAR = \frac{NO_2^- - N_{OUT}}{NO_2^- - N_{OUT} + NO_3^- - N_{OUT}} \quad (2)$$

Nitrogen effluent fractions were calculated according to the literature (Mannina et al., 2016):

$$\text{Nitrified N} = \frac{NH_4^+ - N_{IN} - NH_4^+ - N_{OUT} - N_{metabolic}}{NH_4^+ - N_{IN} - N_{metabolic}} \quad (3)$$

$$\text{Denitrified N} = \frac{NH_4^+ - N_{IN} + NO_x - N_{IN} - NH_4^+ - N_{OUT} - NO_x - N_{OUT} - N_{metabolic}}{NH_4^+ - N_{IN} + NO_x - N_{IN} - N_{metabolic}} \quad (4)$$

Where NO_x is the sum of NO_2^--N and NO_3^--N and $N_{metabolic}$ is 5 % of the sCOD removed.

3. Results and discussion

3.1. Performance of the nitritation reactor

The N-SBR was operated for approximately 130 days, aiming to produce a suitable NO_x load to facilitate the AE/AN enrichment in the S-SBR. Table 4 summarizes the reactor's performance in contaminants removal. The system achieved a high removal efficiency in the first three periods, particularly in period III, where the highest values were

Table 3
Average operational conditions of the selection reactor S-SBR.

Parameter	U.M	Period I	Period II	Period III	Period IV
Influent C/N	g COD g N^{-1}	1.78 ± 0.46	3.13 ± 0.43	3.87 ± 0.45	5.11 ± 1.53
F/M	kg BOD kg SS^{-1} d^{-1}	0.12 ± 0.03	0.18 ± 0.05	0.21 ± 0.05	0.17 ± 0.08
SRT	days	6.38 ± 3.31	5.54 ± 2.61	8.00 ± 6.36	12.03 ± 7.69
OLR	kg COD m^{-3} d^{-1}	0.38 ± 0.12	0.64 ± 0.06	0.75 ± 0.09	0.60 ± 0.23
NLR	kg N m^{-3} d^{-1}	0.21 ± 0.02	0.21 ± 0.01	0.20 ± 0.05	0.12 ± 0.03
COD_{VFA}/NO_x	g COD_{VFA} $g^{-1}NO_x$-N	11.14 ± 6.64	13.55 ± 2.49	20.13 ± 8.37	51.23 ± 13.59
TSS	g L^{-1}	1.28 ± 0.28	1.33 ± 0.33	1.34 ± 0.34	1.35 ± 0.41
VSS	g L^{-1}	0.92 ± 0.16	1.01 ± 0.31	0.99 ± 0.30	1.00 ± 0.34

obtained for sCOD and PO_4^{3-}-P removal. The C/N shift from 2 gCOD $g^{-1}N$ in period I to 4 gCOD $g^{-1}N$ in period III did not result in substantial differences, with the PO_4^{3-}-P removal mainly affected by the lower influent concentrations. However, system efficiency rapidly decreased at C/N higher than 5.5 gCOD $g^{-1}N$. Despite the lower COD influent concentrations, COD removal efficiency decreased, on average, by 10 %. This result may be related to the lower amount of readily biodegradable COD in period IV, which corresponds to the lowest VFA/sCOD ratio recorded (0.27). The removal efficiency trends for NH_4^+-N and NO_x-N are shown in Fig. 2. During period IV, NH_4^+-N removal accounted for, on average, 74.7 ± 14.7 %, with nitrification efficiency and NAR of 45.4 ± 14.6 % and 29.7 ± 4.6 %, respectively. The decline in influent NH_4^+-N concentration resulted in reduced free ammonia levels in the reactor and an increased C/N ratio, conditions that impaired the activity of ammonia-oxidising bacteria (AOB) and created a competitive advantage for nitrite-oxidising bacteria (NOB) (Shao et al., 2018; Okabe et al., 2011). According to part of the literature (Wu et al., 2016), SRT should have been closer to 5 days instead of fostering the AOB's activity. However, some studies report an opposite trend, indicating that high SRTs inhibit NOB activity (Conca et al., 2020; Jubany et al., 2009). However, since the SRT slightly changed during the experimental period, it is reasonable to say that it didn't affect the biological activity in the N-SBR. The nitrification efficiency was consistently higher than 70 % in the previous periods, whereas during period III, the highest NAR value of 54.5 ± 0.6 % was recorded. The NAR values registered are in accordance with previous studies for the NLR adopted in the N-SBR (Frison et al., 2015a, 2015b; Conca et al., 2020) higher NAR registered in period III may be related to the higher temperature recorded during the experimental activity in period III (Table 2).

The system efficiency worsening in period IV is also shown by the N_2O emissions and N effluent fractions reported in Fig. 3. Period I was characterized by the highest emitted N_2O concentration (0.62 ± 0.08 mg N_2O-N L^{-1}) mainly because of the low C/N adopted (2 gCOD $g^{-1}N$) (Mannina et al., 2018b). However, the emission factor was considerably low, at 0.24 ± 0.02 %, highlighting the high biological activity previously reported. Despite the higher nitrite accumulated during period II compared to period I, lower N_2O emission (0.42 ± 0.05 mg N_2O-N L^{-1}) and emission factor (0.19 ± 0.01 %) were achieved. Period III showed higher N_2O emission (0.49 ± 0.03 mg N_2O-N L^{-1}). Since the low difference in C/N ratios, the NAR played a role in the process. During period III, nitrite accounted, on average, for 6.3 ± 1.8 mg N L^{-1}, resulting in the average emission factor of 0.30 ± 0.06 %. As reported in the literature, increased nitrite accumulation will increase N_2O emission during the AOB nitritation process (Massara et al., 2017; Kemmou and Amanatidou, 2023; Law et al., 2012a). Since the nitrite concentration was below 10 mg N L^{-1}, the N_2O emission factor was considerably lower than that reported by Frison et al. (2015a) for around 15 % of the influent TN when nitrite concentration was around 50 mgL^{-1}. While the concentration of emitted N_2O was similar to period III, the period IV emission factor accounted for 0.49 ± 0.08 % of the influent TN. As discussed before and as reported by the lowest nitrified N share in Fig. 2b (53.7 ± 26.5 % of the effluent TN), period IV was characterized by a nitrification disturbance, which maintained the emitted N_2O concentration (0.51 ± 0.03 mg N_2O-N L^{-1}) comparable to period III despite the lower nitrites accumulated. As intermediate compounds in the AOB-mediated N_2O production pathway were not measured, the observed increase in N_2O emissions can only be attributed hypothetically to incomplete oxidation of hydroxylamine (Law et al., 2012b).

Table 4
Average and standard deviation removal efficiencies for the nitritation reactor.

Parameter	sCOD			PO_4^{3-}-P		
U.M	IN mg L^{-1}	OUT mg L^{-1}	Removal %	IN mg P L^{-1}	OUT mg P L^{-1}	Removal %
Period I	215.4 ± 69.6	13.1 ± 3.4	93.3 ± 3.4	21.9 ± 3.8	12.8 ± 1.6	40.9 ± 7.3
Period II	373.8 ± 36.6	12.9 ± 2.3	96.5 ± 0.9	10.5 ± 6.0	6.1 ± 3.7	43.2 ± 9.1
Period III	441.4 ± 62.4	11.4 ± 10.7	97.1 ± 3.2	8.1 ± 4.3	2.7 ± 0.9	59.6 ± 20.7
Period IV	315.8 ± 118.2	44.9 ± 30.0	86.1 ± 7.1	9.7 ± 4.7	3.0 ± 0.9	57.6 ± 31.3

3.2. Performance of the selection reactor

The S-SBR was coupled with an MBR unit to test the feasibility of achieving an effluent which could be reused. Accordingly, effluent COD concentrations were evaluated against the BOD discharge limit of 10 mg L^{-1} set by Regulation 2020/741/EU, while nitrogen and phosphorus concentrations were compared to the thresholds defined by Italian Decree 39/2023, 15 mg L^{-1} for total nitrogen and 2 mg L^{-1} for total phosphorus for WWTPs serving fewer than 100,000 population equivalents. Overall, the system achieved high removal efficiencies for COD and N over the four periods, as reported in Table 5. Contrary to the N-SBR, the COD removal efficiency never dropped below 90 %, meeting the discharge limit for all periods except period IV. As discussed, this period was characterised by a low readily biodegradable COD, which worsened biological activity. TN removal efficiency also remained above 85 %, registering a slight decrease during period IV compared to the previous periods. Still, effluent TN concentration was within the legislation limits for periods II and III. The effluent phosphate concentration never met the legislation limits imposed by ITA/39/2023, thus highlighting the need for further optimisations in this regard. As reported in Fig. 4, no substantial worsening of the ammonia removal occurred during the experimental period. It accounted, on average, for 90.6 ± 3.5 %, 87.5 ± 2.4 %, 91.4 ± 2.3 % and 87.1 ± 3.5 % for periods I, II, III and IV, respectively. Additionally, the denitrification efficiency was stabilised at a value higher than 85 % during the first three periods, indicating that the system was not affected by the C/N shifts from 2 to 4 gCOD $g^{-1}N$ (Wang et al., 2021). However, the severely decreased nitrites and nitrates concentrations in the N-SBR effluent during period IV worsened the S-SBR performance. Indeed, the lowest denitrification efficiency of 22.9 ± 9.7 % was achieved during that period. Overall, a slightly higher denitrification efficiency was achieved in this work compared to other studies that applied the two-reactor scheme (Frison et al., 2015a; Conca et al., 2020; Frison et al., 2015b, 2021). However, it must be noted that a lower NLR was adopted in this work for the S-SBR

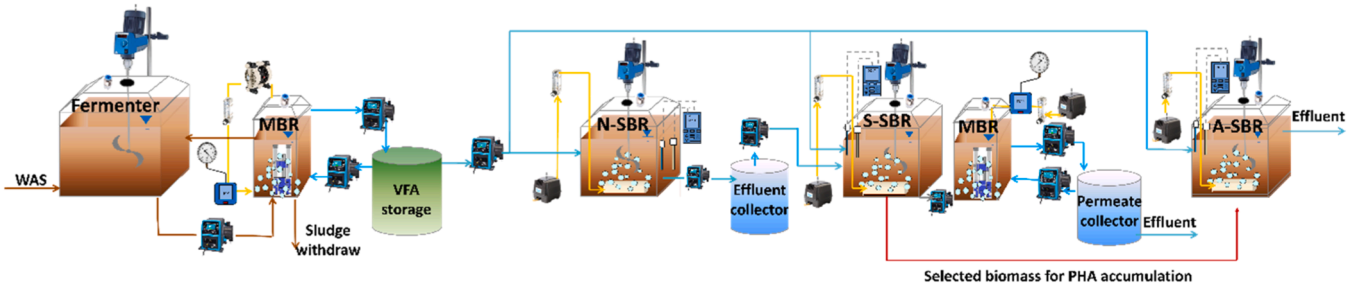

Fig. 1. Schematic view of the adopted layout.

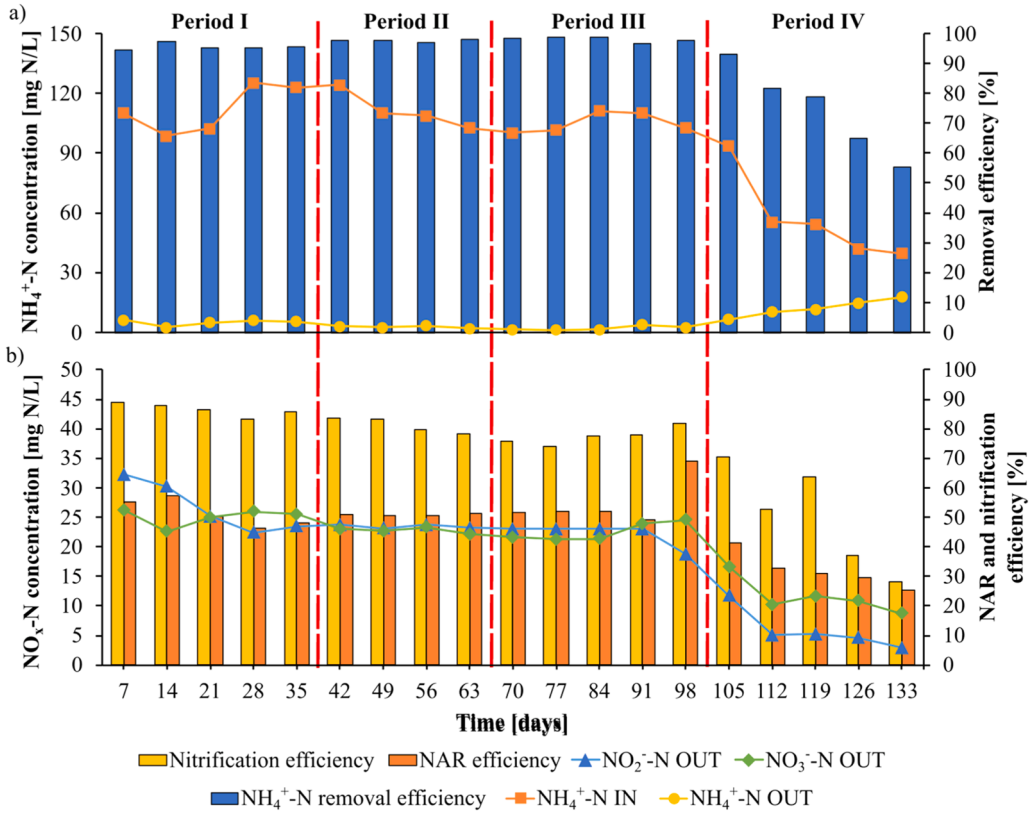

Fig. 2. Ammonia removal efficiency (a), NAR and nitrification efficiencies with the related NO_x species (b) for the nitritation reactor.

operation, 50–70 % lower than the above-cited manuscript, and that a higher COD_{VFA}/NO_x ratio was measured, thus favouring a more effective complete via-nitrite/nitrate nitrogen removal process. The high denitrification efficiency was also not affected by the relatively low NAR efficiency of the N-SBR, thus indicating that there is no substantial difference in using nitrites or nitrates as electron acceptors when PHA is used as an internal carbon source (Liu et al., 2023; Salehizadeh and Van Loosdrecht, 2004). A similar denitrification efficiency was achieved compared to the single reactor process adopted in several literature studies. Still, higher overall nitrogen removal was reported in this work, thus proving the higher efficiency of adopting the N-SBR for complete nitrogen removal (Basset et al., 2016; Tu et al., 2019; Liu et al., 2023). However, as reported in Fig. 3, higher efficiency comes at the cost of higher N_2O emissions and increased indirect emissions due to the setup and operation of an additional reactor (Mannina and Mineo, 2024).

Considering the 2020/741/EU and ITA/39/2023, the system produced a reusable effluent, in addition to the PO_4^{3-}-P concentration. However, considering the proposed new Urban Wastewater Treatment Directive, a lot of work still needs to be done. Suppose the advantage of implementing the PHA production within the WWTP operation wants to be exploited. In that case, further solutions and more advanced treatments must be adopted, or simpler PHA production schemes (i.e., direct accumulation) may be coupled with further nutrient removal processes.

As already reported for the N-SBR, period IV was characterized by low biological activity, which also resulted in higher N_2O emissions in the S-SBR, as reported in Fig. 5. Considering the average emissions during the periods, the N_2O total concentration was always below 0.4 mg N_2O-N L^{-1}. Period I showed the highest concentration of emitted N2O-N, reaching 0.39 ± 0.09 mg N_2O-N L^{-1}, while the lowest was registered during period II (0.24 ± 0.04 mg N_2O-N L^{-1}). Similarly to the N-SBR, the highest concentration reached during period I may be related to a C/N ratio below 2.85 gCOD g^{-1}N, which can result in an electron donor deficiency and lower microbial activity (Santorio et al., 2019). As for the emission factor, periods II and III achieved the lowest level of 0.15 %, while period IV achieved, on average, 0.29 ± 0.05 %. The worsening of the activity during period IV is also shown by the nitrogen effluent fractions reported in Fig. 5b. The denitrified N accounted for approximately 58 % of the effluent N, representing a decrease of around 20 % compared to previous periods. Moreover, the metabolic N share increased by around 15 % compared to previous periods, indicating a

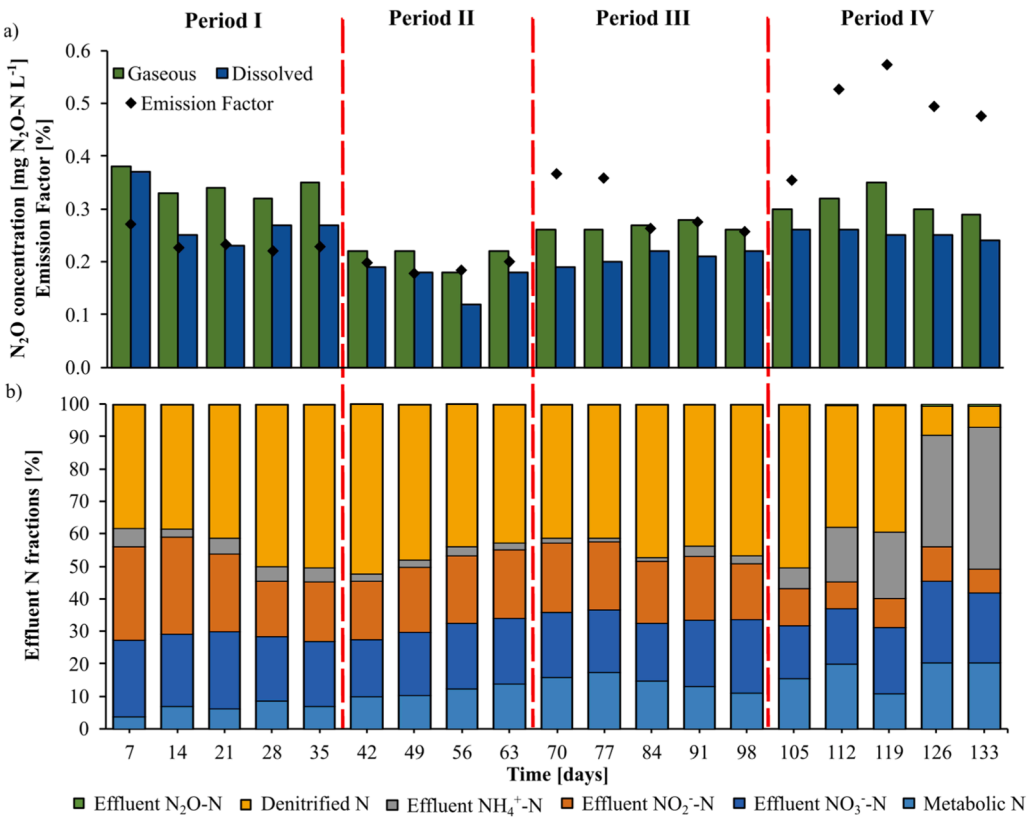

Fig. 3. Gaseous and dissolved N_2O emission and N_2O emission factor measured (a) and effluent nitrogen shares (b) for the nitritation reactor.

Table 5
Average and standard deviation removal efficiencies for the selection reactor S-SBR.

Parameter	sCOD			TN			PO_4^{3-}-P		
	IN	OUT	Removal	IN	OUT	Removal	IN	OUT	Removal
U.M	mg L^{-1}	mg L^{-1}	%	mg N L^{-1}	mg N L^{-1}	%	mg P L^{-1}	mg P L^{-1}	%
Period I	228.5 ± 70.2	6.4 ± 1.6	97.0 ± 1.1	127.3 ± 11.1	11.3 ± 3.4	91.0 ± 3.2	34.7 ± 5.0	18.1 ± 2.9	47.5 ± 8.2
Period II	386.7 ± 35.3	7.7 ± 6.4	98.1 ± 1.4	124.1 ± 8.8	14.5 ± 3.2	88.3 ± 2.3	16.6 ± 9.6	10.0 ± 7.4	44.7 ± 12.0
Period III	452.8 ± 52.8	9.2 ± 4.6	96.1 ± 4.5	117.8 ± 6.3	9.3 ± 2.1	92.1 ± 2.1	10.8 ± 4.0	4.0 ± 1.6	59.3 ± 15.5
Period IV	360.8 ± 139.7	21.0 ± 9.3	93.4 ± 3.3	70.5 ± 18.6	9.6 ± 1.5	85.8 ± 3.7	12.8 ± 4.5	4.7 ± 1.4	61.6 ± 6.0

worsening of heterotrophic activity. In any case, despite the worsening in the last period, N_2O never accounted for more than 0.3 % of the influent N. Different results were reported by Tu et al. (2019) (Tu et al., 2019) which, to the author's knowledge, is the only one monitoring N_2O emissions in an AE/AN enrichment process, besides the authors' studies (Mannina and Mineo, 2024). In their study, the authors conducted denitrification batch tests under anoxic conditions, using a nitrate solution with an initial NO_3-N concentration of 40 ± 3 mg N L^{-1}. The authors reported an average N_2O-N concentration of 2 mg L^{-1}, reaching peaks of around 5 mg L^{-1} at 4 h. The concentration is incredibly higher than that reported in this work, but, at the same time, a higher NO_x concentration is adopted. At the end of the famine step, the authors reported a concentration below 1 mg L^{-1}, highlighting the crucial role of denitrification as an N_2O sink (Conthe et al., 2019) (Fig. 6).

However, the N_2O emission has been poorly addressed in AE/AN enrichment processes compared to other denitrification-based PHA enrichments. As reported by Liu et al. (2015), numerous advanced models were optimized and built upon anaerobic-anoxic processes, which allowed for comprehensive evaluation of the effect of operational parameters (such as the NLR or the SRT), the PHA produced, and the feeding strategy adopted with the N_2O emission (Scherson et al., 2014; Wu et al., 2013). Despite the easy-to-implement process, the AE/AN enrichment still suffers from a knowledge gap that needs to be assessed for scalability.

3.3. *Continuous operation of the accumulation reactor*

The PHA accumulation was carried out continuously in the A-SBR, adopting a feed-on-demand strategy. The reactor operated for 117 days, starting on day 21 of the pilot plant operation. The reactor was fed with wasted enriched biomass produced from the S-SBR on days 29, 45, 76, and 118. Before the inoculum feeding, the biomass within the reactor was withdrawn to maintain a stable TSS concentration of 1 g L^{-1}. The results of the accumulation are reported in Fig. 5.

During the first 80 days of operation, the amount of PHA produced continued to increase with every enriched biomass feeding, reaching a peak concentration of 44.6 % w/w. Of this, 9.9 % w/w was produced as PHV, while the remaining 34.7 % w/w was produced as PHB. The sharp increase registered in the first 30 days of operation was mainly related to PHV production, as the HV:HB peak of 1.04 was achieved on day 28. This result is primarily associated with a high concentration of propionic and valeric acids in the substrate feed, as registered during period I, which is almost comparable to that of acetic acid, as reported in Table 1 (Perez-Zabaleta et al., 2021; Chang et al., 2012; Zhang et al., 2023). Additionally, the sharp increase during the first 30 days was attributed to the highest VFA/sCOD ratio recorded during period I, resulting in a

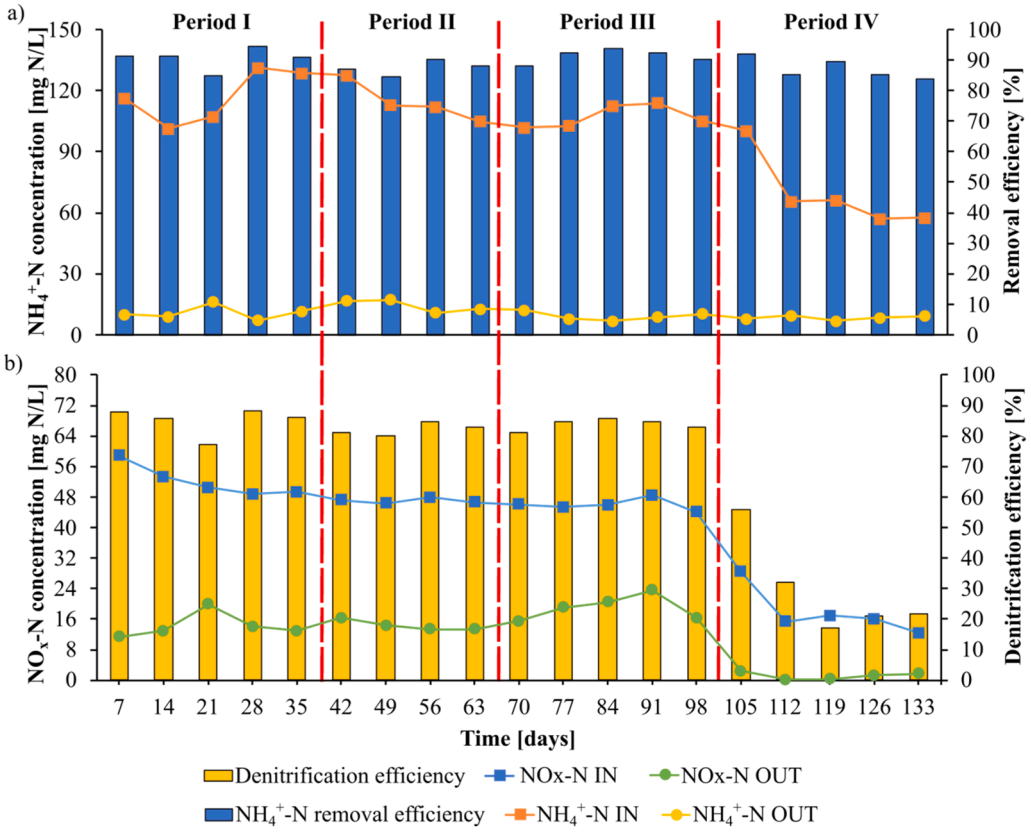

Fig. 4. Ammonia removal efficiency (a) and denitrification efficiency with the relative NO_x trend (b) for the selection reactor.

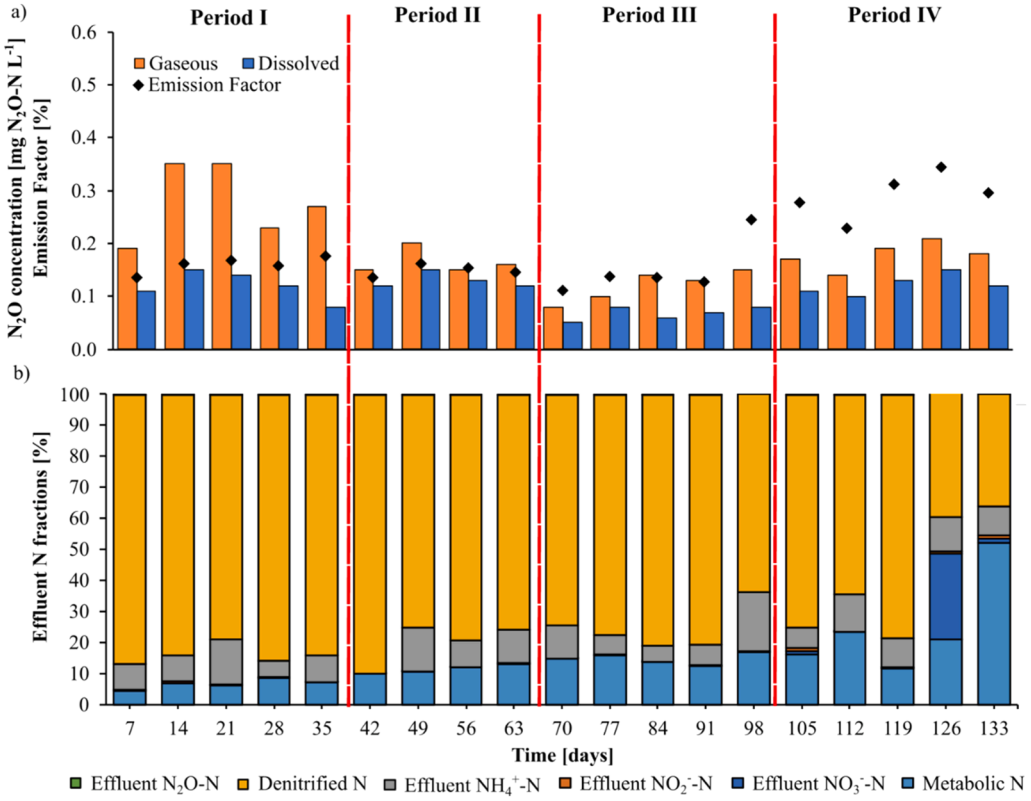

Fig. 5. Gaseous and dissolved N_2O emission and N_2O emission factor measured (a) and effluent nitrogen shares (b) for the selection reactor.

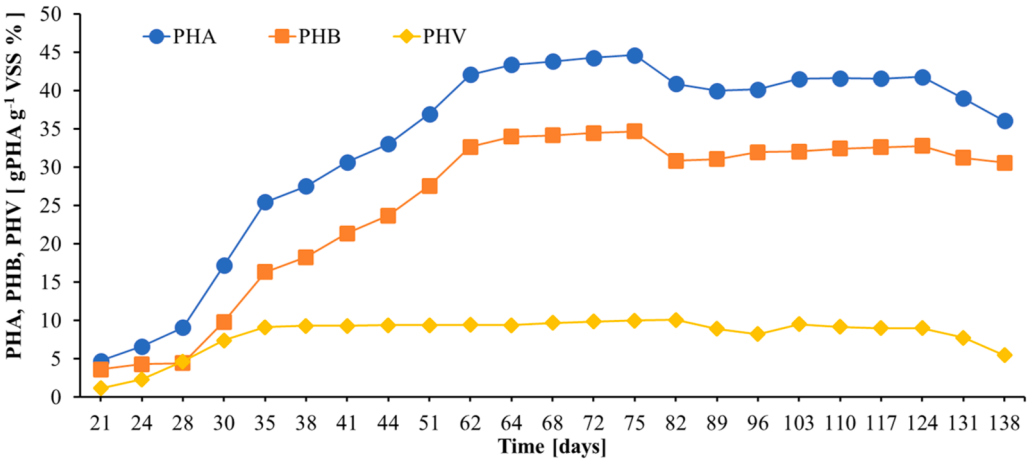

Fig. 6. Trend of PHB, PHV and PHA concentrations measured during the accumulation reactor operation.

storage yield of 0.32 g COD_{PHA} $g^{-1}COD_{VFA}$ (days 20–28). Instead, despite the following periods being characterised by a lower VFA/sCOD ratio, a higher OLR, F/M, SRT, and C/N were measured during periods II and III, which probably resulted in an enriched culture with increased PHA production capacity (Frison et al., 2021; Chen et al., 2017; Mokhtarani et al., 2012; Crognale et al., 2022; Isern-Cazorla et al., 2023). Indeed, the storage yields accounted for 0.53, 0.52, and 0.51 g COD_{PHA} $g^{-1}COD_{VFA}$ on days 29–45, 46–76, and 77–117, respectively. At the same time, despite being characterized by the highest C/N ratio in period IV, the severely decreased VFA/sCOD ratio may have played a crucial role in not increasing the PHA production, achieving an average of 39.6 ± 2.5 % w/w and a storage yield of 0.41 g COD_{PHA} $g^{-1}COD_{VFA}$ during days 117–138. Despite system fluctuations, the A-SBR achieved a stable PHA production of 40–44 % w/w between days 62 and 138. This result slightly contrasts with the relative literature, where the AE/AN is usually considered a low-PHA production strategy (Kourmentza et al., 2017). However, the long-term continuous operation of the accumulation reactor's study showed that a stable PHA production of around 40 % w/w can be achieved. To comprehensively compare the results of this study with the literature, the accumulation results of studies adopting the same enrichment strategy are summarised in Table 6.

The single reactor nitritation-denitritation proposed by Tu et al. (2019) and (Liu et al., 2023) achieved higher PHA concentrations than those reported by Frison et al. (2015a), (2015b) and Conca et al. (2020) adopting a two-reactor process. However, it must be considered that a lower SRT was applied in the selection reactor by Tu et al. (2019) and that a synthetic substrate was used by Liu et al. (2023), which may have favoured PHA production compared to the real substrate. The two reactors' process showed an increased storage yield, which highlights the higher efficiency of the process in enriching the PHA producers' culture. The results presented in this study demonstrate that it is possible to adopt WAS as a feedstock for producing PHA, achieving results similar to those obtained with other more efficient feedstocks typically used in the literature. Moreover, it is worth noting that the lowest C/N ratio during accumulation was adopted in this study, compared to the literature (Table 6), which further underscores the robustness and efficiency of the process. However, it is worth noting that the studies by Frison and Conca involved accumulation over hours, whereas this study was conducted over several days. As indicated by the storage yields obtained, similar to the literature, the difference is primarily related to the feedstock used and its VFA concentration.

3.4. Assessing the possible implementation in WWTP

The recently proposed Urban Wastewater Treatment Directive includes the following recommendations: tertiary treatment for N and P removal for urban areas with > 100,000 person equivalents (PE), the introduction of limits for nitrogen (<6 mg L^{-1}) and phosphorus (<0.5 mg L^{-1}) and the setting up of minimum yields for their removal, 85 % for N and 90 % for P. New standards will be applied for agglomerations of 10,000 PE or more affected by eutrophication by the end of 2040. However, most WWTPs are not designed to meet these legislative limits, indicating that worldwide-scale plant retrofitting may occur soon. To foster the WRRF application, the PHA production process may represent an attractive, sustainable, and efficient process that can be integrated into existing WWTPs to meet future stricter legislative limits. The results presented in this work suggest that AE/AN enrichment may be considered in light of the above.

During the aerobic feast phase, ammonium is partially oxidised to nitrite, providing an electron acceptor that is readily available for the anoxic famine phase. Subsequently, under substrate limitation conditions (anoxic famine), PHA accumulated during the aerobic feast phase acts as an internal carbon reserve, utilized by denitrifying bacteria as an electron donor for nitrite reduction. The internal carbon-driven

Table 6
Operational conditions adopted and results achieved from literature studies that employ the AE/AN enrichment strategy, both as a single reactor and a double reactor.

PHA % w/w	Storage Yield g COD_{PHA} $g^{-1}COD_{VFA}$	Accumulation C/N gCOD g^{-1} N	Selection OLR kg COD m^{-3} d^{-1}	Selection SRT days	Feedstock used	Reference
19–21	0.40	10–13	0.72–0.82	12–15	PS + WAS (thickened) WSFL - SFL	(Frison et al., 2015a)
10–20 (C_{mmol}/C_{mmol})	0.60–0.67	3–5	1.12–1.32	15	Primary + WAS	(Frison et al., 2015b)
44.1	0.58–0.61	50	1.31–1.58	6–7	PS + WAS (normal or thickened)	(Conca et al., 2020)
10.6	0.01–0.22	18–22	0.20–0.26	25	OFMSW - OFMSW + PS	(Basset et al., 2016)
49.7	0.47	7.8	-	4	PS + WAS (thermal-hydrolyzed)	(Tu et al., 2019)
58–64	-	10–20	-	15	Synthetic substrate	(Liu et al., 2023)
40–44	0.32–0.53	2–6	0.38–0.75	5–12	WAS	This study

PS: primary sludge; WSFL: sewage sludge fermentation liquid with wallosonite; SFL: sewage sludge fermentation liquid; OFMSW: organic fraction of municipal solids waste.

denitritation process is particularly advantageous because it avoids external carbon dosing, contributing to overall process economy and operational simiplicity. Considering the effluent legislation limits, high COD and TN removal efficiencies were achieved (>85 %) despite the effluent N values being greater than 6 mg L^{-1}. To decrease the N effluent concentration, the S-SBR denitrification process needs to be improved, either by increasing the length of the famine step or by increasing the amount of PHA produced during the feast to provide a sufficient carbon source for completely consuming the NOx species. Furthermore, as proposed in the literature (Frison et al., 2015a, 2015b, 2021), an N-rich effluent, such as that from an anaerobic digester, can be used in the N-SBR to increase overall efficiency. At the same time, this approach may increase the N_2O emissions, as reported for different enrichment strategies (Liu et al., 2015). Indeed, despite the low N_2O emissions reported in this work, further studies should address the active N_2O generation pathways in the process and evaluate the effectiveness of mitigation strategies, if needed. Since only this study and the one by Tu et al. (2019) have monitored the N_2O emissions of an AE/AN enrichment process, further research is needed, despite the promising results. At the same time, adopting a two-reactor process will inevitably increase the indirect GHG emissions despite the higher N removal efficiency (Mannina and Mineo, 2024). This will lead to further assessment to balance the emissions or improve the efficiency of the single-reactor process. Further studies should also focus on enhancing P removal by implementing chemical reactions or biochar adsorption in the process scheme (Di Capua et al., 2022; Bunce et al., 2018).

The process also achieved stable and continuous PHA accumulation, highlighting the effectiveness of aerobic feast/anoxic famine conditions in selecting and maintaining a consortium enriched with denitrifying, PHA-storing microorganisms. Although microbial community composition was not directly analyzed, the operational results strongly suggest an enriched microbial community capable of both PHA storage and nitrite reduction under the provided operational conditions. Once the nutrient removal is optimised, the system could represent a sustainable and effective alternative to recover both water eligible for reuse and carbon as a biopolymer, thus positively impacting environmental protection and potentially increasing revenue to WWTPs.

4. Conclusions

For the first time, this study demonstrated the feasibility and effectiveness of an MBR-based AE/AN enrichment process adopting WAS from WWTPs operating in continuous conditions. The observed mechanism, driven by internally stored PHA consumption during the anoxic famine, was close to achieving water of effluent quality suitable for reuse. COD removal efficiencies exceeded 90 %, except during period IV, and nitrogen concentrations were below 15 mg L^{-1} for periods II and III, which aligns with EU standards. However, further optimizations are needed to comply with stricter future regulations. Enhancing S-SBR denitrification and integrating nitrogen-rich anaerobic digester effluent may improve performance, though it could increase N_2O emissions in the N-SBR. N_2O emissions pathways and potential mitigation strategies need to be evaluated for the AE/AN enrichment, given the need to enhance its sustainability. The continuous PHA accumulation reactor achieved a considerable PHA accumulation (40–44 % w/w) over the last 76 days. Future work should optimise the process within the WWTP by integrating other treatment steps as necessary, while always managing both direct and indirect GHG emissions. Generally, the environmental aspect of the process is sacrificed in favour of maximizing the amount of PHA produced. However, the future may open novel possibilities for integration within the WWTPs' operation if the environmental impact is considered.

CRediT authorship contribution statement

Antonio Mineo: Writing – original draft, Methodology, Formal analysis, Data curation. **Mark M.C. van Loosdrecht:** Writing – review & editing, Visualization, Validation. **Giorgio Mannina:** Writing – review & editing, Visualization, Validation, Supervision, Funding acquisition, Conceptualization.

Declaration of Competing Interest

The authors declare that they have no known competing financial interests or personal relationships that could have appeared to influence the work reported in this paper.

References

Awasthi, M.K., Ganeshan, P., Gohil, N., Kumar, V., Singh, V., Rajendran, K., Harirchi, S., Solanki, M.K., Sindhu, R., Binod, P., Zhang, Z., Taherzadeh, M.J., 2023. Advanced approaches for resource recovery from wastewater and activated sludge: a review. Bioresour. Technol. 384, 129250. https://doi.org/10.1016/j.biortech.2023.129250.

Basset, N., Katsou, E., Frison, N., Malamis, S., Dosta, J., Fatone, F., 2016. Integrating the selection of PHA storing biomass and nitrogen removal via nitrite in the main wastewater treatment line. Bioresour. Technol. 200, 820–829. https://doi.org/10.1016/j.biortech.2015.10.063.

Bunce, J.T., Ndam, E., Ofiteru, I.D., Moore, A., Graham, D.W., 2018. A review of phosphorus removal technologies and their applicability to Small-Scale domestic wastewater treatment systems. Front. Environ. Sci. 6. ⟨https://www.frontiersin.org/journals/environmental-science/articles/10.3389/fenvs.2018.00008⟩.

Chang, H.-F., Chang, W.-C., Tsai, C.-Y., 2012. Synthesis of poly(3-hydroxybutyrate/3-hydroxyvalerate) from propionate-fed activated sludge under various carbon sources. Bioresour. Technol. 113, 51–57. https://doi.org/10.1016/j.biortech.2011.12.138.

Chaudhry, W.N., Jamil, N., Ali, I., Ayaz, M.H., Hasnain, S., 2011. Screening for polyhydroxyalkanoate (PHA)-producing bacterial strains and comparison of PHA production from various inexpensive carbon sources. Ann. Microbiol. 61, 623–629. https://doi.org/10.1007/s13213-010-0181-6.

Chen, Z., Huang, L., Wen, Q., Zhang, H., Guo, Z., 2017. Effects of sludge retention time, carbon and initial biomass concentrations on selection process: from activated sludge to polyhydroxyalkanoate accumulating cultures. J. Environ. Sci. 52, 76–84. https://doi.org/10.1016/j.jes.2016.03.014.

Conca, V., da Ros, C., Valentino, F., Eusebi, A.L., Frison, N., Fatone, F., 2020. Long-term validation of polyhydroxyalkanoates production potential from the sidestream of municipal wastewater treatment plant at pilot scale. Chem. Eng. J. 390, 124627. https://doi.org/10.1016/j.cej.2020.124627.

Conthe, M., Lycus, P., Arntzen, M., Ramos da Silva, A., Frostegård, Å., Bakken, L.R., Kleerebezem, R., van Loosdrecht, M.C.M., 2019. Denitrification as an N_2O sink. Water Res. 151, 381–387. https://doi.org/10.1016/j.watres.2018.11.087.

Crognale, S., Lorini, L., Valentino, F., Villano, M., Cristina, M.G., Barbara, T., Majone, M., Rossetti, S., 2022. Effect of the organic loading rate on the PHA-storing microbiome in sequencing batch reactors operated with uncoupled carbon and nitrogen feeding. Sci. Total Environ. 825, 153995. https://doi.org/10.1016/j.scitotenv.2022.153995.

Di Capua, F., de Sario, S., Ferraro, A., Petrella, A., Race, M., Pirozzi, F., Fratino, U., Spasiano, D., 2022. Phosphorous removal and recovery from urban wastewater: current practices and new directions. Sci. Total Environ. 823, 153750. https://doi.org/10.1016/j.scitotenv.2022.153750.

European Parliament, Directive (EU) 2024/3019 of the European Parliament and of the Council of 27 November 2024 concerning urban wastewater treatment, (2024).

Frison, N., Andreolli, M., Botturi, A., Lampis, S., Fatone, F., 2021. Effects of the sludge retention time and carbon source on Polyhydroxyalkanoate-Storing biomass selection under Aerobic-Feast and Anoxic-Famine conditions. ACS Sustain Chem. Eng. 9, 9455–9464. https://doi.org/10.1021/acssuschemeng.1c02973.

Frison, N., Katsou, E., Malamis, S., Oehmen, A., Fatone, F., 2015a. Development of a novel process integrating the treatment of sludge reject water and the production of polyhydroxyalkanoates (PHAs). Environ. Sci. Technol. 49, 10877–10885. https://doi.org/10.1021/acs.est.5b01776.

Frison, N., Katsou, E., Malamis, S., Oehmen, A., Fatone, F., 2015b. Nutrient removal via nitrite from reject water and polyhydroxyalkanoate (PHA) storage during nitrifying conditions. J. Chem. Technol. Biotechnol. 90, 1802–1810. https://doi.org/10.1002/jctb.4487.

Guo, R., Cen, X., Ni, B.-J., Zheng, M., 2024. Bioplastic polyhydroxyalkanoate conversion in waste activated sludge. J. Environ. Manag. 370, 122866. https://doi.org/10.1016/j.jenvman.2024.122866.

He, L., Rosa, L., 2023. Solutions to agricultural Green water scarcity under climate change. PNAS Nexus 2, pgad117. https://doi.org/10.1093/pnasnexus/pgad117.

Isern-Cazorla, L., Mineo, A., Suárez-Ojeda, M.E., Mannina, G., 2023. Effect of organic loading rate on the production of polyhydroxyalkanoates from sewage sludge. J. Environ. Manag. 343, 118272. https://doi.org/10.1016/j.jenvman.2023.118272.

Jubany, I., Lafuente, J., Baeza, J.A., Carrera, J., 2009. Total and stable washout of nitrite oxidizing bacteria from a nitrifying continuous activated sludge system using automatic control based on oxygen uptake rate measurements. Water Res. 43, 2761–2772. https://doi.org/10.1016/j.watres.2009.03.022.

Kemmou, L., Amanatidou, E., 2023. Factors affecting nitrous oxide emissions from activated sludge wastewater treatment plants—a review. Resources 12. https://doi.org/10.3390/resources12100114.

Kourmentza, C., Plácido, J., Venetsaneas, N., Burniol-Figols, A., Varrone, C., Gavala, H. N., Reis, M.A.M., 2017. Recent advances and challenges towards sustainable polyhydroxyalkanoate (PHA) production. Bioengineering 4. https://doi.org/10.3390/bioengineering4020055.

Kowal, P., Mehrani, M.J., Sobotka, D., Ciesielski, S., Mąkinia, J., 2022. Rearrangements of the nitrifiers population in an activated sludge system under decreasing solids retention times. Environ. Res. 214. https://doi.org/10.1016/j.envres.2022.113753.

Law, Y., Ni, B.-J., Lant, P., Yuan, Z., 2012b. N2O production rate of an enriched ammonia-oxidising bacteria culture exponentially correlates to its ammonia oxidation rate. Water Res. 46, 3409–3419. https://doi.org/10.1016/j.watres.2012.03.043.

Law, Y., Ye, L., Pan, Y., Yuan, Z., 2012a. Nitrous oxide emissions from wastewater treatment processes. Philos. Trans. R. Soc. B Biol. Sci. 367, 1265–1277. https://doi.org/10.1098/rstb.2011.0317.

Liu, Y., Peng, L., Guo, J., Chen, X., Yuan, Z., Ni, B.-J., 2015. Evaluating the role of microbial internal storage turnover on nitrous oxide accumulation during denitrification. Sci. Rep. 5, 15138. https://doi.org/10.1038/srep15138.

Liu, B., Wen, Q., Huang, L., Chen, Z., Lin, X., Liu, S., 2023. Insights into integration of polyhydroxyalkanoates (PHAs) production into wastewater treatment: comparison of different electron acceptors on system function and PHA-producer enrichment. Chem. Eng. J. 451. https://doi.org/10.1016/j.cej.2022.138631.

Mannina, G., Alduina, R., Badalucco, L., Barbara, L., Capri, F.C., Cosenza, A., Di Trapani, D., Gallo, G., Laudicina, V.A., Muscarella, S.M., Presti, D., 2021. Water resource recovery facilities (Wrrfs): the case study of palermo university (Italy). Water 13. https://doi.org/10.3390/w13233413.

Mannina, G., Capodici, M., Cosenza, A., Di Trapani, D., Ekama, G.A., 2018a. Solids and hydraulic retention time effect on N_2O emission from Moving-Bed membrane bioreactors. Chem. Eng. Technol. 41, 1294–1304. https://doi.org/10.1002/ceat.201700377.

Mannina, G., Cosenza, A., Di Trapani, D., Capodici, M., Viviani, G., 2016. Membrane bioreactors for treatment of saline wastewater contaminated by hydrocarbons (diesel fuel): an experimental pilot plant case study. Chem. Eng. J. 291, 269–278. https://doi.org/10.1016/j.cej.2016.01.107.

Mannina, G., Ekama, G.A., Capodici, M., Cosenza, A., Di Trapani, D., Ødegaard, H., van Loosdrecht, M.M.C., 2018b. Influence of carbon to nitrogen ratio on nitrous oxide emission in an integrated fixed film activated sludge membrane BioReactor plant. J. Clean. Prod. 176, 1078–1090. https://doi.org/10.1016/j.jclepro.2017.11.222.

Mannina, G., Mineo, A., 2024. A comprehensive comparison between two strategies to produce polyhydroxyalkanoates from domestic sewage sludge. J. Clean. Prod. 468, 143052. https://doi.org/10.1016/j.jclepro.2024.143052.

Mannina, G., Presti, D., Montiel-Jarillo, G., Suárez-Ojeda, M.E., 2019. Bioplastic recovery from wastewater: a new protocol for polyhydroxyalkanoates (PHA) extraction from mixed microbial cultures. Bioresour. Technol. 282, 361–369. https://doi.org/10.1016/j.biortech.2019.03.037.

Massara, T.M., Malamis, S., Guisasola, A., Baeza, J.A., Noutsopoulos, C., Katsou, E., 2017. A review on nitrous oxide (N_2O) emissions during biological nutrient removal from municipal wastewater and sludge reject water. Sci. Total Environ. 106–123. https://doi.org/10.1016/j.scitotenv.2017.03.191.

Mineo, A., Isern-Cazorla, L., Rizzo, C., Piccionello, A.P., Suárez-Ojeda, M.E., Mannina, G., 2023. Polyhydroxyalkanoates production by an advanced food-on-demand strategy: the effect of operational conditions. Chem. Eng. J. 472. https://doi.org/10.1016/j.cej.2023.145007.

Mineo, A., van Loosdrecht, M.M.C., Mannina, G., 2024. Assessing the aerobic/anoxic enrichment efficiency at different C/N ratios: pilot scale polyhydroxyalkanoates production from waste activated sludge. Water Res., 122687 https://doi.org/10.1016/j.watres.2024.122687.

Mineo, A., van Loosdrecht, M.M.C., Mannina, G., 2025. From waste activated sludge to polyhydroxyalkanoate: insights from a membrane-based enrichment process. Chem. Eng. J. 506, 160089. https://doi.org/10.1016/j.cej.2025.160089.

Mokhtarani, N., Ganjidoust, H., Vasheghani Farahani, E., 2012. Effect of process variables on the production of polyhydroxyalkanoates by activated sludge. Iran. J. Environ. Health Sci. Eng. 9, 6. https://doi.org/10.1186/1735-2746-9-6.

Montiel-Jarillo, G., Gea, T., Artola, A., Fuentes, J., Carrera, J., Suárez-Ojeda, M.E., 2021. Towards PHA production from wastes: the bioconversion potential of different activated sludge and food industry wastes into VFAs through acidogenic fermentation. Waste Biomass. Valoriz. 12, 6861–6873. https://doi.org/10.1007/s12649-021-01480-4.

Okabe, S., Aoi, Y., Satoh, H., Suwa, Y., 2011. Nitrification in wastewater treatment. Nitrification 405–433. https://doi.org/10.1128/9781555817145.ch16.

Perez-Zabaleta, M., Atasoy, M., Khatami, K., Eriksson, E., Cetecioglu, Z., 2021. Bio-based conversion of volatile fatty acids from waste streams to polyhydroxyalkanoates using mixed microbial cultures. Bioresour. Technol. 323, 124604. https://doi.org/10.1016/j.biortech.2020.124604.

Rice, E.W., Bridgewater, Laura, 2012. American public health association., American water works association., water environment federation. Standard Methods for the Examination of Water and Wastewater. American Public Health Association.

Salehizadeh, H., Van Loosdrecht, M.C.M., 2004. Production of polyhydroxyalkanoates by mixed culture: recent trends and biotechnological importance. Biotechnol. Adv. 22, 261–279. https://doi.org/10.1016/j.biotechadv.2003.09.003.

Santorio, S., Fra-Vázquez, A., Val del Rio, A., Mosquera-Corral, A., 2019. Potential of endogenous PHA as electron donor for denitrification. Sci. Total Environ. 695, 133747. https://doi.org/10.1016/j.scitotenv.2019.133747.

Scherson, Y.D., Woo, S.-G., Criddle, C.S., 2014. Production of nitrous oxide from anaerobic digester centrate and its use as a Co-oxidant of biogas to enhance energy recovery. Environ. Sci. Technol. 48, 5612–5619. https://doi.org/10.1021/es501009j.

Shao, Y., Yang, S., Mohammed, A., Liu, Y., 2018. Impacts of ammonium loading on nitritation stability and microbial community dynamics in the integrated fixed-film activated sludge sequencing batch reactor (IFAS-SBR). Int. Biodeterior. Biodegrad. 133, 63–69. https://doi.org/10.1016/j.ibiod.2018.06.002.

Tsuneda, S., Mikami, M., Kimochi, Y., Hirata, A., 2005. Effect of salinity on nitrous oxide emission in the biological nitrogen removal process for industrial wastewater. J. Hazard Mater. 119, 93–98. https://doi.org/10.1016/j.jhazmat.2004.10.025.

Tu, W., Zhang, D., Wang, H., Lin, Z., 2019. Polyhydroxyalkanoates (PHA) production from fermented thermal-hydrolyzed sludge by PHA-storing denitrifiers integrating PHA accumulation with nitrate removal. Bioresour. Technol. 292, 121895. https://doi.org/10.1016/j.biortech.2019.121895.

Wang, H., Chen, N., Feng, C., Deng, Y., 2021. Insights into heterotrophic denitrification diversity in wastewater treatment systems: progress and future prospects based on different carbon sources. Sci. Total Environ. 780. https://doi.org/10.1016/j.scitotenv.2021.146521.

Wu, J., He, C., van Loosdrecht, M.C.M., Pérez, J., 2016. Selection of ammonium oxidizing bacteria (AOB) over nitrite oxidizing bacteria (NOB) based on conversion rates. Chem. Eng. J. 304, 953–961. https://doi.org/10.1016/j.cej.2016.07.019.

Wu, G., Zhai, X., Jiang, C., Guan, Y., 2013. Effect of ammonium on nitrous oxide emission during denitrification with different electron donors. J. Environ. Sci. 25, 1131–1138. https://doi.org/10.1016/S1001-0742(12)60164-8.

Yuan, Q., Sparling, R., Oleszkiewicz, J.A., 2011. VFA generation from waste activated sludge: effect of temperature and mixing. Chemosphere 82, 603–607. https://doi.org/10.1016/j.chemosphere.2010.10.084.

Zhang, W., Alvarez-Gaitan, J.P., Dastyar, W., Saint, C.P., Zhao, M., Short, M.D., 2018. Value-Added products derived from waste activated sludge: a biorefinery perspective. Water 10. https://doi.org/10.3390/w10050545.

Zhang, Z., Lin, Y., Wu, S., Li, X., Cheng, J.J., Yang, C., 2023. Effect of composition of volatile fatty acids on yield of polyhydroxyalkanoates and mechanisms of bioconversion from activated sludge. Bioresour. Technol. 385, 129445. https://doi.org/10.1016/j.biortech.2023.129445.

Zhang, X., Liu, Y., 2022. Resource recovery from municipal wastewater: a critical paradigm shift in the post era of activated sludge. Bioresour. Technol. 363, 127932. https://doi.org/10.1016/j.biortech.2022.127932.